

**Evolution of Active Galaxies:
Black-hole Mass – Bulge relations for Narrow Line Objects**

Smita Mathur¹

Astronomy Department, The Ohio State University, Columbus, OH 43210

smita@astronomy.ohio-state.edu

Joanna Kuraszkiewicz

Harvard-Smithsonian Center for Astrophysics, Cambridge, MA 02138

joasia@head-cfa.harvard.edu

and

Bozena Czerny

N. Copernicus Astronomical Center, Warsaw, Poland

bcz@camk.edu.pl

ABSTRACT

Mathur (2000) has proposed that the narrow line Seyfert 1 galaxies (NLS1s) are likely to be the active galaxies in early stage of evolution. To test this hypothesis, we have calculated the black hole (BH) masses and the host galaxy bulge masses for a sample of NLS1s. We find that the mean BH to bulge mass ratio of NLS1s is significantly smaller than that for normal Seyfert galaxies. We also find that the ratio of BH mass to bulge velocity dispersion is also significantly smaller for NLS1s. A scenario of BH growth is our preferred interpretation, though alternative explanations are discussed. Assuming that the BHs grow with accretion with a radiative efficiency of 0.1, it will take them $t \gtrsim 3.3 \times 10^8$ years to become as massive as in normal Seyfert 1s. These timescales are consistent with the theoretical estimates of quasar timescale $t_Q \lesssim 4.5 \times 10^8$ years calculated by Haehnelt, Natarajan & Rees (1998). Studies of low redshift NLS1s thus provide a powerful, and due to their proximity relatively easy, way to understand the high redshift quasars and their evolution.

Subject headings: galaxies:active - galaxies: evolution - quasars: general - galaxies: Seyfert

¹Harvard-Smithsonian Center for Astrophysics, Cambridge, MA 02138

1. Introduction

Last couple of years have seen significant progress in our understanding of the relationship between quasar activity and galaxy formation. In the framework of the hierarchical dark-matter cosmogony (e.g. Haehnelt, Natarajan & Rees 1998, HNR98 hereafter), the formation and evolution of galaxies and their active nuclei is intimately related (Fabian 1999, Granato *et al.* 1999, Haehnelt & Kauffmann 1999). It is assumed that the supermassive black holes form proportionally to the dark matter halos. The process of formation of a massive BH and the active nucleus is the very process of galaxy formation. The active nucleus and the galaxy evolve together, with BH accreting matter and the galaxy making stars. At one stage the winds from the active nucleus blow away the matter surrounding it and a quasar emerges. This is not only the end of active evolution of the quasar but that of the galaxy as well, which is evacuated of its interstellar medium. The quasar then shines as long as there is fuel in the accretion disk (Fabian 1999). In this scenario, high-redshift quasars represent the early stage of galaxy evolution, BALQSOs at $z \approx 2$ represent the stage when the gas is being blown away, and $z \approx 1$ quasars would be the passively evolving population. Massive ellipticals found today might be the dead remnants of what were once luminous quasars.

Observational support to the above scheme of evolution is also accumulating. In a classic paper, Maggorian *et al.* (1998) found that the mass of a BH in the nucleus of a galaxy is correlated with the mass of its bulge (see also van der Marel *et al.* 1999 and an excellent review by Richstone *et al.* 1998). Most recently, Gebhardt *et al.* (2000a) and Ferrarese & Merritt (2000) found a correlation between the BH mass and the bulge velocity dispersion, a much tighter relation than that between the BH mass and bulge luminosity. The important point to note is that the nuclear BH seems to “know” the galaxy it harbors. Laor (1998) showed that the above correlation for normal galaxies extends to quasar host galaxies as well. The similarity of the two correlations is remarkable given the widely different levels of BH activity in luminous quasars and nearby massive normal galaxies. Franceschini *et al.* (1999) found an interesting similarity between the evolution rates for the total populations of galaxies and AGNs. By comparing the evolution of star formation rate per comoving volume in galaxies and the volume emissivity by AGNs, they found that the evolution of luminous quasars parallels that of stellar populations in massive spheroidal galaxies.

Much of the above observational evidence relates BH masses of luminous quasars, or what were once luminous quasars, with spheroidal masses of massive galaxies. Wandel (1999) extended Laor’s work to low redshift Seyfert galaxies for which BH masses were available using reverberation mapping. Interestingly, Wandel (1999) found that the average BH- to bulge-mass ratio for Seyferts is systematically lower than that for normal galaxies and luminous quasars. Wandel interpreted this result as a scenario of BH growth in which a BH in a Seyfert grows by accretion to become a more massive BH in a quasar. This, however, is highly unlikely since the Seyferts are known to accrete at a sub-Eddington rate while the luminous quasars in Laor’s sample accrete at close to Eddington rate. So, in the above scenario, the accretion rate has to grow with time, which is difficult to achieve and contrary to theoretical expectations. A possible explanation of the Laor and Wandel results might be that the quasars and Seyferts represent two different populations (Mathur

2000). The quasar phenomenon may be a result of galaxy formation due to primordial density fluctuations or mergers at early cosmic epochs, which were to result in massive ellipticals of today. At low redshifts, when new galaxies are formed due to interactions or mergers, similar evolution may take place. Gebhardt *et al.* (2000b) have now found that the Seyferts and normal galaxies have the same BH mass–bulge velocity dispersion relationship. Note, however, that it still implies that the Seyferts are different from the normal galaxies in that the bulges of Seyferts have lower mass to light ratio, unless the Wandel result is purely due to observational uncertainty.

While we now have the observational evidence for a relation between an AGN and its host galaxy, we do not know how it got there, or what are the evolutionary steps towards the “final” correlation discussed above. Mathur (2000) has argued that narrow line Seyfert 1 galaxies (NLS1s) may represent an early phase in the evolution of active galaxies at low redshift. In our scenario, the luminous quasars and the low-luminosity Seyferts follow separate but similar evolutionary tracks. In both cases the accretion rate $\dot{m} = \dot{M}/\dot{M}_{Eddington}$ is large in the early stages of evolution and reduces later on, consistent with the theoretical expectations (e.g. HNR98). To test this hypothesis, we determine the BH- to bulge-mass relation as well as the BH-mass to bulge velocity dispersion relation for NLS1s and compare those with the normal Seyfert relation. In §2 we detail our method and present interpretation in §3.

2. BH and Bulge Relations for NLS1s

2.1. Determination of BH Mass

Our sample consists of 15 narrow-line AGN (11 NLS1s and 4 NL quasars) for which soft- and hard X-ray spectra are available in literature. The central black hole masses for these objects were calculated by fitting their spectral energy distributions with the accretion disk and corona (ADC) model of Witt, Czerny & Życki (1997) (see Kuraszek *et al.* 2000 for details). In this model the corona accretes and generates energy through viscosity, and the division between optically thin accretion flow (corona) and optically thick flow (disk) results from the cooling instability discussed by Krolik, McKee and Tarter (1981). The model is fully described by the following parameters: the mass of the central black hole, accretion rate and viscosity parameter. The calculated black hole masses are quoted in Table 1.

We determine the errors of the black hole mass estimated from spectral fitting as follows. The fit is based on two relations: (1) the asymptotic shape of the disk emission in the optical band is: $F_\nu \propto \nu^{1/3}(M\dot{M})^{2/3}\cos i H_0^2 f^{-4/3}$, where M is mass of the black hole, \dot{M} - accretion rate, i - the inclination angle of the disk, H_0 is the Hubble constant, f - spectral correction given by color temperature to the effective temperature ratio; (2) the bolometric luminosity is: $F_{bol} \propto \dot{M}\eta H_0^2$, where η is the efficiency of accretion. In our fits we adopt the following values: $H_0 = 50$ km/s/Mpc, $\cos i = 1$, $f = 1$ and $\eta = 1/16$. If any of these values are different, the mass of the black hole would scale as: $M_{real} = M_{calc} f^2 (\cos i)^{-1} (H_0/50)^{-1}$. The inclination angle of the disk for Seyfert 1s is in

the range 0° to 48° (Schmitt et al. 2000 and assuming the accretion disk is aligned with the dusty torus), the upper limit for f is 1.7 (Róžańska, private communication), and if there is strong outflow close to the black hole η decreases (up to a factor 2 if the outflow is energetically comparable to the outflows in radio-loud objects). Taking all these effects into account we estimate the calculated mass of the black hole to be accurate to ${}^{+0.64}_{-0.30}$ in logarithm.

For the sake of consistency and comparison with earlier results, we also calculated the BH masses for the 7 Sy1s from Wandel’s sample, for which X-ray spectra were available. The results are presented in Table 2. The calculated black hole masses are compared to the virial masses in Tables 2 and 3. The masses calculated by the ADC model are generally larger than masses estimated by Wandel. We calibrate our BH mass determinations with the virial mass estimates for the objects in Table 2 and 3 and find that: $\log M_{\text{bh}}^{\text{calib}} = \log M_{\text{bh}}^{\text{calc}} - 0.70 \pm 0.15$. This relation, together with the calculated and virial BH masses for Seyfert 1s and NLS1s (excluding the outlying point for IC 4329A²), is displayed in Figure 1. It can be clearly seen that the above equation is a good description of the relation between BH masses calculated by the ADC model and by the virial method. There is clearly some uncertainty in the ADC mass estimates, as discussed above (Tables 1, 2, 3), and the virial mass estimates are also uncertain by a factor of several because of the uncertainty in the geometry of the broad emission line region. Both of these effects contribute towards the scatter seen in Figure 1. The calibrated black hole masses for NLS1s are given in Table 3. These masses were used to calculate the black hole to bulge mass ratio.

2.2. Determination of Bulge Mass

For the NLS1s in our sample, we determined the bulge masses of their host galaxies following the general method used by Laor (1998) and Wandel (1999), which we discuss briefly below. For most of our NLS1s we obtain the bulge absolute blue magnitudes ($M_{\text{B}}^{\text{bulge}}$) from Whittle (1992). A galaxy’s total blue magnitude ($M_{\text{B}}^{\text{total}}$) is related to $M_{\text{B}}^{\text{bulge}}$ by Simien & Vaucouleurs (1986) equation (for $H_0 = 50 \text{ km s}^{-1} \text{ Mpc}^{-1}$, $q_0 = 0$): $M_{\text{B}}^{\text{total}} - M_{\text{B}}^{\text{bulge}} = 0.324\tau - 0.054\tau^2 + 0.0047\tau^3$ where $\tau = T + 5$ and T is the Hubble stage (defined in de Vaucouleurs, de Vaucouleurs & Corwin 1976).

Mrk 110 and Mrk 335 do not have a Hubble type defined in the Whittle (1992) compilation. However NED³ quotes a S0/a Hubble type for Mrk 335, which we use to calculate the bulge

²The virial mass for IC 4329A is adopted from Wandel 1999 who has adopted it from Wandel, Peterson & Malkan 1999. We find that IC 4329A is an outlier in all the relations discussed in Wandel, Peterson & Malkan 1999 as well as in Peterson *et al.* 2000. This leads us to suspect the virial BH mass of this object. We ignore IC 4329A in rest of the paper.

³This research has made use of the NASA/IPAC Extragalactic Database (NED) which is operated by the Jet Propulsion Laboratory, California Institute of Technology, under contract with the National Aeronautics and Space Administration.

magnitude for this object. The resulting M_B^{bulge} (Table 3) is consistent with that in Ho (1999). For Mrk 110 we adopt a canonical Hubble type of Sa.

For NAB 0205+024, PG 1402+261 and PG 1444+407 we take the host galaxy absolute magnitudes from Bahcall et al. (1997), which have been corrected for nuclear emission. For Mrk 1044 we take the host galaxy magnitude from MacKenty (1990), who has nuclear emission included in the total blue magnitude, hence in Table 3 we quote the bulge mass as an upper limit.

After obtaining the bulge blue magnitudes we use the relation between the bulge B and V magnitude (Worthey 1994) $B-V=0.95$, the standard relation between the bulge luminosity and absolute magnitude: $\log(L_{\text{bulge}}/L_{\odot}) = 0.4(-M_V^{\text{bulge}} + 4.83)$ and the relation between bulge mass and bulge luminosity for normal galaxies from Magorrian et al. (1998): $\log M_{\text{bulge}}/M_{\odot} = -1.11 + 1.18 \log L_{\text{bulge}}/L_{\odot}$. The bulge masses calculated this way are listed in Table 3.

2.3. Determination of Bulge Velocity Dispersion

We do not have bulge velocity dispersion (σ_*) measurements for the objects in our sample. However, Nelson (2000) has shown that the width of the narrow emission line [OIII] serves as a good representation of the velocity dispersion with $\sigma_* = \text{FWHM [OIII]}/2.35$. Adopting from Nelson (2000), we collected from literature, as well as from our optical data, the values of FWHM [OIII] for all the NLS1s in our sample (Osterbrock & Pogge 1985, Wamsteker *et al.* 1985, Dahari & De Robertis 1988, Busko & Steiner 1988, Nelson & Whittle 1995, Wilkes *et al.* 1999).

3. Results and Discussion

3.1. BH- to Bulge-mass relation for NLS1s

In Figure 2 we have plotted the log of BH mass vrs. log of bulge mass obtained using the method discussed in §2. The dashed line represents the relation for normal galaxies and luminous quasars (from Laor 1998) while the dotted line represents the relation for Seyfert galaxies (from Wandel 1999, excluding 3 NLS1s in his sample; we have also re-calculated the bulge masses for these objects, as Wandel uses a slightly different relation between the mass and luminosity of the bulge than we do). The NLS1s are represented by filled squares. It is immediately apparent that the relation for Seyfert galaxies does not hold for NLS1s; NLS1s lie systematically below the line for Seyfert galaxies. In addition, we find that the narrow line quasars also lie systematically below the line for quasars. The mean $M_{\text{BH}}/M_{\text{bulge}}$ for NLS1s is 0.00005, lower by a factor of six compared to $M_{\text{BH}}/M_{\text{Bulge}} = 0.0003$ for Wandel’s Seyferts, excluding the three NLS1s in his sample. Similarly, the BH to bulge mass ratio for NL quasars is 0.0005, almost an order of magnitude lower than 0.006 for normal galaxies and quasars.

We would like to emphasize that, since we have calibrated our BH masses with those from the reverberation mapping, the relative difference in the BH- to bulge-mass relation of NLS1s and normal Sy1s is a robust result, though the absolute values may suffer from various uncertainties. We have not been able to do such a calibration for NL quasars, so we cannot place similar confidence in the difference between NL quasars and the quasars in Laor’s sample.

Comparison of BH mass to bulge mass, using bulge luminosity, is a worthwhile exercise even in the light of the new, stronger, correlation with bulge velocity dispersion. Reasons for the differences in two correlations may be many: e.g. Hubble types of many bright AGNs may have systematic errors, or nuclear starbursts may reduce the mass to light ratio of bulges in AGNs (Gebhardt *et al.* 2000b). Understanding these differences is important. Moreover, here we are comparing two subclasses of Seyfert galaxies: regular, broad line Seyfert 1s and NLS1s, so any systematic problems in determining the bulge luminosity is likely to be the same in both classes. So, any difference in the two is not likely to be a result of observational uncertainty.

3.2. BH-mass to Bulge-velocity dispersion relation for NLS1s

Nelson (2000) has determined BH-mass to bulge velocity dispersion relation for Seyfert galaxies. It is noteworthy that all the three NLS1s in his sample: NGC 4051, Mkn 110, and Mkn 335, lie at the lowest boundary of the scatter. In figure 3 we have plotted the log of BH mass vrs FWHM [OIII]/2.35. The open squares are the Seyfert 1s and the filled circles are the NLS1s in our sample. The straight line represents the relation for Seyfert galaxies from Nelson (2000). While the Seyfert 1s follow the Nelson relation, NLS1s lie systematically below the line.

3.3. Interpretation

The above results support our conjecture that NLS1s are young AGNs. NLS1s are believed to accrete at close to Eddington rate, as first proposed by Pounds, Done & Osborn (1995). As discussed earlier, in our scenario the accretion rate is highest in the early growing stage of an AGN. The BH would grow by accretion and eventually the accretion rate would slow down. Whether the bulge mass would grow or not would depend upon how young/ rejuvenated the galaxy is, or how complete is the interaction/ merger. So an AGN will follow a vertically upward or diagonally upward (with both M_{BH} and M_{Bulge} increasing) track on Figure 2, as it evolves. Similarly, if the bulge velocity dispersion has settled down to its “final” value, an AGN would follow a vertically upward track on Figure 3.

An alternative interpretation of the BH- to bulge-mass relation might be that the bulge mass to light ratio in NLS1s is lower compared to normal Seyferts (see §1). This might be due to higher bulge luminosity as a result of a nuclear starburst, again supporting our proposal of NLS1s being rejuvenated AGN (Mathur 2000). This, however, cannot explain the result regarding velocity

dispersion. Alternatively, the above results might mean that the bulge luminosities and FWHM [OIII] are systematically overestimated for NLS1s. While not impossible, it seems unlikely that both the quantities are overestimated.

Assuming that our results are not just due to observational uncertainties, and that our scenario of BH growth is valid, some interesting inferences may be obtained. It can be seen from figure 2 that for NLS1s, the relation between BH mass and bulge mass is not strictly linear. So, the BH mass is not a “universal fraction” of the baryonic mass as suggested by Haiman & Loeb (1998). More likely, the accretion process determines the BH mass (e.g. HNR99) at any given time. The Salpeter time for the growth of a BH, i.e. the e-folding time, is $t_s = 4 \times 10^7 (L_{Eddington}/L)\eta_{0.1}$ years where $\eta_{0.1}$ is the radiative efficiency normalized to 0.1. $L/L_{Eddington}$ calculated for the objects in our sample is listed in Table 1. For a bulge with mass $\approx 10^{11}M_\odot$, we have a BH mass of $5 \times 10^6M_\odot$ for NLS1 Mrk 493. (Figure 2, Table 3). Let us assume this to be the initial BH mass. The BH would grow to a “final” Seyfert mass of $\sim 5 \times 10^7M_\odot$ assuming $M_{BH}/M_{Bulge} = 0.00047$. So to grow by a factor of 10, a BH would need $2.3t_s = 3.3 \times 10^8\eta_{0.1}$ years, for a constant accretion rate. Since the accretion rate decreases with time, the growth time scale $t \gtrsim 3.3 \times 10^8\eta_{0.1}$ years.

It is possible that being more luminous, quasars evolve faster than the Seyferts. However, if the evolution of quasars and of Seyferts is indeed similar, then quasar lifetimes of about 10^8 years is inferred. This timescale is much larger than $\sim 10^6$ yr. proposed by Haiman & Loeb (1998). HNR98 predict quasar lifetimes anywhere in the range 10^6 to 10^8 yrs. Our results are consistent with, and close to their upper limit $t_Q \lesssim 4.5 \times 10^8\eta_{0.1}$ years calculated for $L/L_{Eddington} = 1.0$. HNR98 have considered three different scenarios for BH growth in a quasar: (i) accretion far above the Eddington rate, (ii) accretion obscured by dust, and (iii) accretion below the critical rate leading to an advection dominated accretion flow lasting for a Hubble time. Our results, together with Laor (1998) make the third option unlikely. For NLS1s, we have evidence for accretion rate close to Eddington rate, but not far above the Eddington rate. There are also several NLS1s which are dusty (e.g. IRAS 13349+2438). So options (i) and (ii) are plausible. Studies of low redshift NLS1s thus provide a unique and relatively easy way to understand the high redshift quasars and their evolution.

We gratefully acknowledge financial support through NASA grant NAG5-8913 (LTSA to SM) and NAG5-3363task22 (JK).

REFERENCES

- Bahcall, J. N., Kirhakos, S., Saxe, D. H., & Schneider, D. P. 1997, ApJ, 479, 642
- Boller, Th., Brandt, W.N., & Fink, H. 1996, A&A, 305, 53
- Busko, I.C. & Steiner, J.E. 1988, MNRAS, 232, 525

- de Vaucouleurs, G., de Vaucouleurs, A., & Corwin, H.G., Jr. 1976, *The Second Reference Catalogue of Bright Galaxies* (Austin: Univ. Texas Press)
- Dahari, O. & De Robertis, M. 1988, *ApJS*, 67,249
- Fabian, A.C. 1999, *MNRAS*, 308, L39
- Ferrarese, L. & Merritt, D. 2000, *ApJ*, 539, L9
- Fiore, F., Elvis, M., Siemiginowska, A., Wilkes, B. J., McDowell, J. C., & Mathur, S. 1995, *ApJ*, 449, 74
- Fiore, F., Matt, G., Cappi, M., Elvis, M., Leighly, K. M., Nicastro, F., Piro, L., Siemiginowska, A., & Wilkes, B. J. 1998, *MNRAS*, 298, 103
- Franceschini, A., Hasinger, G., Miyaji, T., & Malquori, D. 1999, *MNRAS Letters*, 310, L5
- Gebhardt, K. *et al.* 2000a, astro-ph/0006289
- Gebhardt, K. *et al.* 2000b, astro-ph/0007123
- Granato, G.L., Silva, L., Monaco, P., Panuzzo, P., Salucci, P., De Zotti, G., & Danese, L. 1999 *MNRAS*, submitted (astro-ph/9911304)
- Grupe, D., Wills, Beverley J., Wills, D., & Beuermann, K. 1998, *AA*, 333, 827
- Haehnelt, M. & Kauffmann, G. 2000, *MNRAS*, 318, L35
- Haehnelt, M., Natarajan, P. & Rees, M. 1998 *MNRAS*, 300, 817 (HNR98)
- Haiman, Z. & Loeb, A. 1998, *ApJ*, 503, 505
- Ho, L. 1999 in “Observational Evidence for Black Holes in the Universe”, Ed: S. Chakrabarti (Dordrecht: Kluwer)
- Krolik, J. H., McKee, C. F., & Tarter, C. B. 1981, *ApJ*, 249, 422
- Kuraszkiewicz, J., Wilkes, B.J., Czerny, B., & Mathur, S. 2000, *ApJ*, 542, 692
- Laor, A., Fiore, F., Elvis, M., Wilkes, B. J., & McDowell J. C. 1997, *ApJ*, 477, 93
- Laor, A. 1998, *ApJL*, 505, 83
- Lawson, A. J., & Turner, M. J. L. 1997, *MNRAS*, 288, 920
- MacKenty, J. W. 1990, *ApJS*, 72, 231
- Magorrian, J., Tremaine, S., Richstone, D., Bender, R., Bower G., Dressler, A., Faber, S. M., Gebhardt, K., Green, R., Grillmair, C., Kormendy, J. & Lauer T. 1998, *ApJ*, 115, 2285

- Malkan, M. A., Gorjian, V., & Tam, R. 1998, *ApJS*, 117, 25
- Mathur, S. 2000, *MNRAS Letters*, 314, L17
- Nandra, K., & Pounds, K.A. 1994, *MNRAS*, 268, 405
- Nandra, K., George, I. M., Mushotzky, R. F., Turner, T. J., & Yaqoob, T. 1997, *ApJ*, 477, 602
- Nelson, C. H. & Whittle, M. 1995, *ApJS*, 99, 67
- Nelson, C. H. 2000, *ApJL*, 545, 91
- Osterbrock, D. & Pogge, R. 1985, *ApJ*, 297, 166
- Peterson, B.M. *et al.* 2000, *ApJ*, 542, 161
- Pounds, K., Done, C., & Osborne, J., 1995 *MNRAS*, 277, L5
- Read, A. M., & Pietsch, W., 1998, *A&A*, 336, 855
- Richstone, D. *et al.* 1998, *astro-ph/9810378*
- Reynolds, C. S. 1997, *MNRAS*, 286, 513
- Schmitt, H.R., Antonucci, R.R., Ulvestad, J.S., Kinney, A.L., Clarke, C.J., & Pringle, J.E., 2001, *ApJ*, in press (*astro-ph/0103263*)
- Simien, F., & de Vaucouleurs, G. 1986, *ApJ*, 302, 564
- Turner, T. J., Nandra, K., George, I. M., Fabian, A. C., & Pounds, K. A. 1993, *ApJ*, 419, 127,
- van der Marel, R. P. 1999 in ‘Galaxy Interactions at Low and High Redshift’, *Proceedings of IAU Symposium 186*, held at Kyoto, Japan, 26-30 August, 1997. Ed: J. E. Barnes, and D. B. Sanders. Kluwer Academic Publishers, Dordrecht/Boston/London, 1999., p.333
- Wamsteker, W. *et al.* 1985, *ApJ*, 295, L33
- Wandel, A. 1999, *ApJL*, 519, 39
- Wandel, A., Peterson, B.M., & Malkan, M. 1999, *ApJ*, 526, 579
- Wang, T.-G., Lu, Y.-J. & Zhou, Y.-Y. 1998, *ApJ*, 483, 1
- Wang, T., Brinkmann W., & Bergeron J. 1996, *A&A*, 309, 81
- Whittle, M. 1992, *ApJS*, 79, 49
- Wilkes, B.J. *et al.* , 1999, *ApJ*, 513, 76
- Witt, H. J. Czerny, B., & Życki, P. T. 1997, *MNRAS*, 286, 848

Worthey, G. 1994, ApJS, 95, 107

Figure Captions:

Figure 1: *log* of BH masses estimated by reverberation mapping is plotted against that calculated with ADC model. Filled symbols are for Seyfert 1s and the open symbols are for NLS1s. The straight line represents the relation between the two mass estimates (see text).

Figure 2: BH mass plotted against bulge mass. The NLS1s, represented by filled squares lie systematically below the dotted line describing the Seyfert relation.

Figure 3: BH mass plotted against the bulge velocity dispersion. Seyfert 1s are represented by open squares and NLS1s by filled circles. The straight line describes the AGN relation from Nelson (2000).

TABLE 1
NLS1 BEST FIT MODEL PARAMETERS:

Name	$\log M_{bh}^a$	L/L_{Edd}^b	α_{softX}^c	α_{ROSAT}^d	Ref.	α_{hardX}^e	α_{ASCA}^f	Ref.	$\log \nu L_\nu(2500\text{\AA})^g$
Mrk 335	7.63	0.40	1.97	1.92±0.04	1	1.16	1.05 ^{+0.14} _{-0.23}	7	44.45
Mrk 359	7.22	0.30	1.37	1.4±0.1	2	2.81	43.87
NAB 0205+024	8.45	0.27	2.50	2.8±0.5	3	1.04	1.09±0.10	8	45.24
Mrk 1044	7.20	0.24	2.06	2.0±0.1	2	1.14	43.79
Mrk 110	7.48	0.40	1.34	1.35±0.05	1	2.84	44.11
Mrk 1239	7.31	0.27	2.60	2.9±0.3	2	1.10	43.94
Mrk 42	7.06	0.29	1.56	1.6±0.2	2	2.74	43.67
NGC 4051	6.27	0.01	1.89	1.86±0.06	1	1.25	1.11±0.08	7	42.48
Mrk 766	7.29	0.26	1.68	1.5±0.2	2	1.17	1.16 ^{+0.15} _{-0.11}	7	43.90
PG 1402+261	8.56	0.40	1.94	1.93±0.03	4	1.06	45.49
PG 1444+407	8.52	0.27	1.94	1.91±0.05	4	1.06	45.44
Mrk 493	7.42	0.28	1.76	1.7±0.2	2	2.36	44.07
II Zw 136	8.20	0.27	1.51	1.25±...	5	1.11	1.17±0.07 ^h	9	45.04
Ark 564	7.57	0.25	2.46	2.4±0.1	2	1.04	44.22
Mrk 1126	6.90	0.29	1.57	1.5±...	6	2.75	43.45

a: Calculated black hole mass in solar masses accurate to within $^{+0.64}_{-0.30}$.

b: Luminosity to the Eddington luminosity ratio.

c: Calculated soft X-ray index measured from 0.1-2.5 keV corresponding to a ROSAT slope.

d: Observed ROSAT (0.1-2.5keV) spectral index.

e: Hard X-ray index measured from 2-10 keV corresponding to an ASCA slope.

f: Observed ASCA (2-10keV) spectral index.

g: Obtained from observed V magnitude assuming slope $\alpha = -0.5$ ($f_\nu \propto \nu^\alpha$), and $H_0 = 50 \text{ km s}^{-1} \text{ Mpc}^{-1}$, $q_0 = 0$.

h: Slope from *Ginga* determined between 2-18keV.

References for ROSAT and ASCA slopes: 1 - Wang, Brinkmann & Bergeron (1996); 2 - Boller, Brandt & Fink (1996); 3 - Fiore et al. (1995); 4 - Laor et al. (1997); 5 - Wang, Lu & Zhou (1998); 6 - Gruppe et al. (1998); 7 - Nandra et al. (1997); 8 - Fiore et al. (1998); 9 - Lawson & Turner (1997).

TABLE 2
BEST FIT MODEL PARAMETERS FOR SEYFERT 1 GALAXIES:

Name	$\log M_{bh}^a$	$\log M_{bh}^b$ virial	α_{softX}^c	α_{ROSAT}^d	Ref.	α_{hardX}^e	α_{ASCA}^f	Ref.	$\log \nu L_\nu(2500A)^g$
Fairall 9	8.42	$7.94_{-0.32}^{+0.11}$	1.43	1.42 ± 0.05	1	1.05	$1.02_{-0.18}^{+0.10}$	5	45.10
PG 0953+414	9.00	$8.19_{-0.38}^{+0.23}$	1.55	2.57 ± 0.03	4	1.08	46.00
NGC 3783	8.16	$7.04_{-1.04}^{+0.30}$	1.06	1.15 ± 0.21	3	1.00	$0.77_{-0.06}^{+0.08}$	5	43.56
IC 4329A	9.84	<6.86	0.83	0.73 ± 0.33	2	0.84	$0.84_{-0.01}^{+0.01}$	6	43.93
NGC 5548	8.15^h	$7.83_{-0.07}^{+0.10}$
Mrk 509	8.37	$7.98_{-0.03}^{+0.14}$	1.59	1.58 ± 0.10	1	1.00	$0.98_{-0.02}^{+0.02}$	8	45.03
NGC 7469	8.31	$6.88_{-...}^{+0.30}$	1.09	1.38 ± 0.05	1	1.02	$0.91_{-0.08}^{+0.09}$	5	44.26

a: Calculated black hole mass in solar masses accurate to within $_{-0.30}^{+0.64}$.

b: Virial mass calculated by Wandel (1999).

c: Calculated soft X-ray index measured from 0.1-2.5 keV corresponding to a ROSAT slope.

d: Observed ROSAT (0.1-2.5 keV) spectral index.

e: Hard X-ray index measured from 2-10 keV corresponding to an ASCA slope.

f: Observed ASCA (2-10 keV) spectral index.

g: Obtained from observed V magnitude assuming slope $\alpha = -0.5$ ($f_\nu \propto \nu^\alpha$), and $H_0 = 50 \text{ km s}^{-1} \text{ Mpc}^{-1}$, $q_0 = 0$.

h: Black hole mass calculated by Kuraszkiewicz et al. (1997).

References for ROSAT and ASCA slopes: 1 - Wang, Lu & Zhou (1998); 2 - Read & Pietsch, (1998); 3 - Turner et al. (1993); 4 - Laor et al. (1997); 5 - Nandra et al. (1997); 6 - Nandra & Pounds (1994); 7 - Lawson & Turner (1997); 8 - Reynolds (1997).

TABLE 3
NLS1 CENTRAL BLACK HOLE MASSES

Name	Type	$-M_B^a$	Ref. ^b	$\log M_{bulge}$	$\log M_{bh}$ virial ^c	Ref. ^b	$\log M_{bh}$ calc. ^d	$\log M_{bh}$ calib. ^e	$\log M_{bh}/M_{bulge}$	Notes
Mrk 335	S0/a	20.33 ± 0.6	1	11.21 ± 0.24	$6.59^{+0.13}_{-0.14}$	5	7.63	$6.93^{+0.64}_{-0.30}$	-4.28	
Mrk 359	SB0	20.52 ± 0.4	1	11.30 ± 16	7.22	$6.52^{+0.64}_{-0.30}$	-4.78	
NAB 0205+024	S0?	20.44 ± 0.2	2	11.27 ± 0.08	7.55	6	8.45	$7.75^{+0.64}_{-0.30}$	-3.52	QSO
Mrk 1044 ^f	SB0	20.4 ± 0.5	3	<11.24	7.20	$6.50^{+0.64}_{-0.30}$	> -4.74	
Mrk 110	-	20.76 ± 1.0	1	11.42 ± 0.40	$6.90^{+0.14}_{-0.20}$	5	7.48	$6.78^{+0.64}_{-0.30}$	-4.64	
Mrk 1239	E/S0	20.19 ± 0.4	1	11.15 ± 0.16	7.31	$6.61^{+0.64}_{-0.30}$	-4.54	
Mrk 42	SBb	18.51 ± 0.4	1	10.36 ± 0.16	7.06	$6.36^{+0.64}_{-0.30}$	-4.00	
NGC 4051	SABbc	19.70 ± 0.2	1	10.91 ± 0.08	$6.15^{+0.30}_{-0.45}$	5	6.27	$5.57^{+0.64}_{-0.30}$	-5.34	
Mrk 766	SBa	20.10 ± 0.2	1	11.10 ± 0.08	7.29	$6.59^{+0.64}_{-0.30}$	-4.51	
PG 1402+261	SBb	21.06 ± 0.2	2	11.56 ± 0.08	7.84	6	8.56	$7.86^{+0.64}_{-0.30}$	-3.70	QSO
PG 1444+407	E1	21.66 ± 0.2	2	11.85 ± 0.08	8.16	6	8.52	$7.82^{+0.64}_{-0.30}$	-4.03	QSO
Mrk 493	SBb	$18.94 \pm \dots$	4	$10.56 \pm \dots$	7.42	$6.72^{+0.64}_{-0.30}$	-3.84	
II Zw 136	S	21.98 ± 0.6	1	11.99 ± 0.24	8.20	$7.50^{+0.64}_{-0.30}$	-4.49	QSO
Ark 564	SBb	20.11 ± 0.4	1	11.11 ± 0.16	7.57	$6.87^{+0.64}_{-0.30}$	-4.24	
Mrk 1126	SBa	18.96 ± 0.4	1	10.57 ± 0.16	6.90	$6.20^{+0.64}_{-0.30}$	-4.37	

a: Absolute blue magnitude of the galactic bulge, (nuclear emission is subtracted); $H_0 = 50 \text{ km s}^{-1} \text{ Mpc}^{-1}$, and $q_0 = 0.0$.

b: References: 1 - Whittle (1992); 2 - Bahcall, Kirhakos & Saxe (1997); 3 - MacKenty (1990); 4 - Malkan, Gorjian & Tam (1998); 5 - Wandel (1999); 6 - Laor (1998).

c: Virial black hole mass from literature.

d: Black hole mass calculated from our accretion disk and corona model accurate to within 0.01.

e: Calibrated black hole mass = $\log M_{bh}$ calc. -0.70 ± 0.15 .

f: M_B includes nuclear emission, hence the estimated bulge mass is an upper limit.

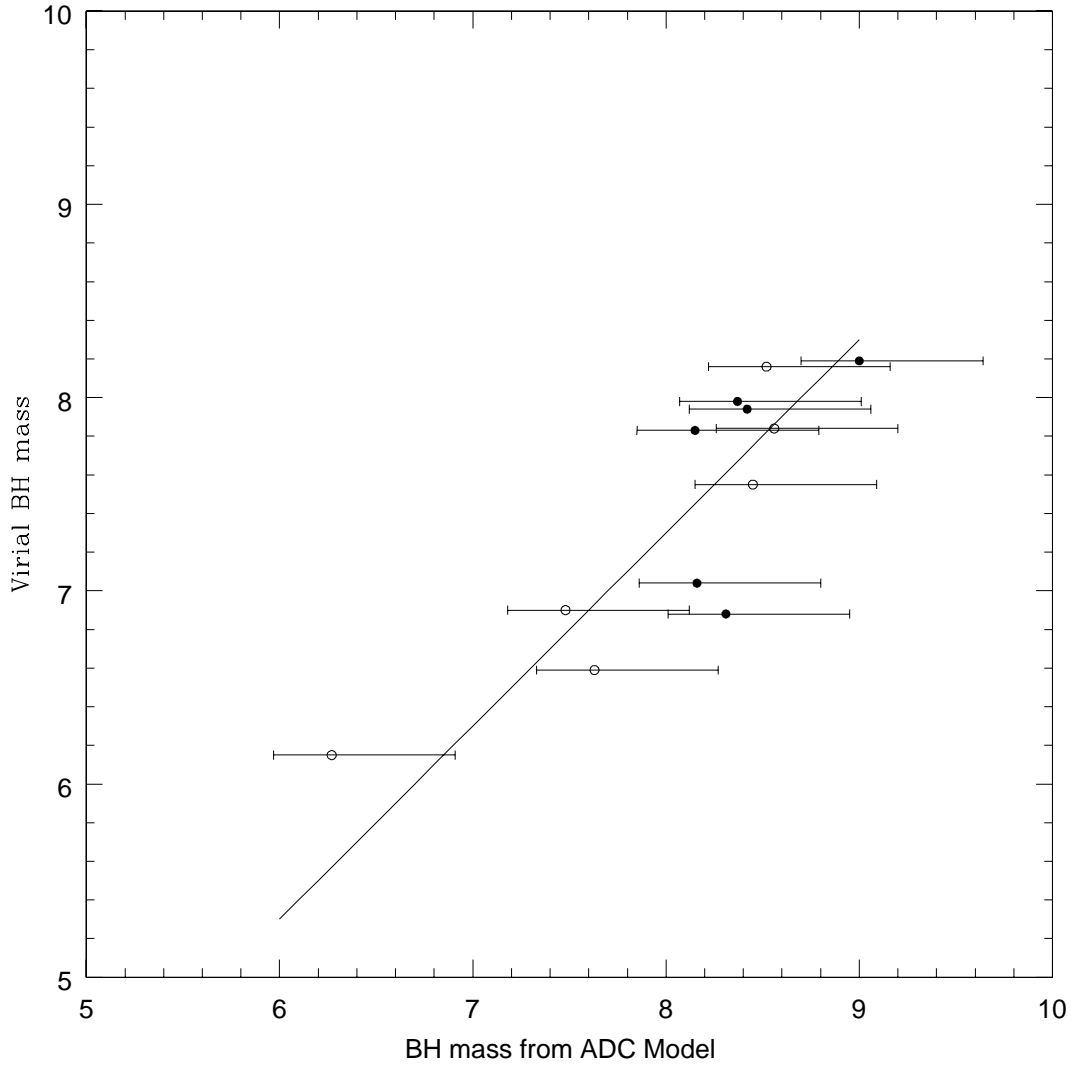


Fig. 1.—

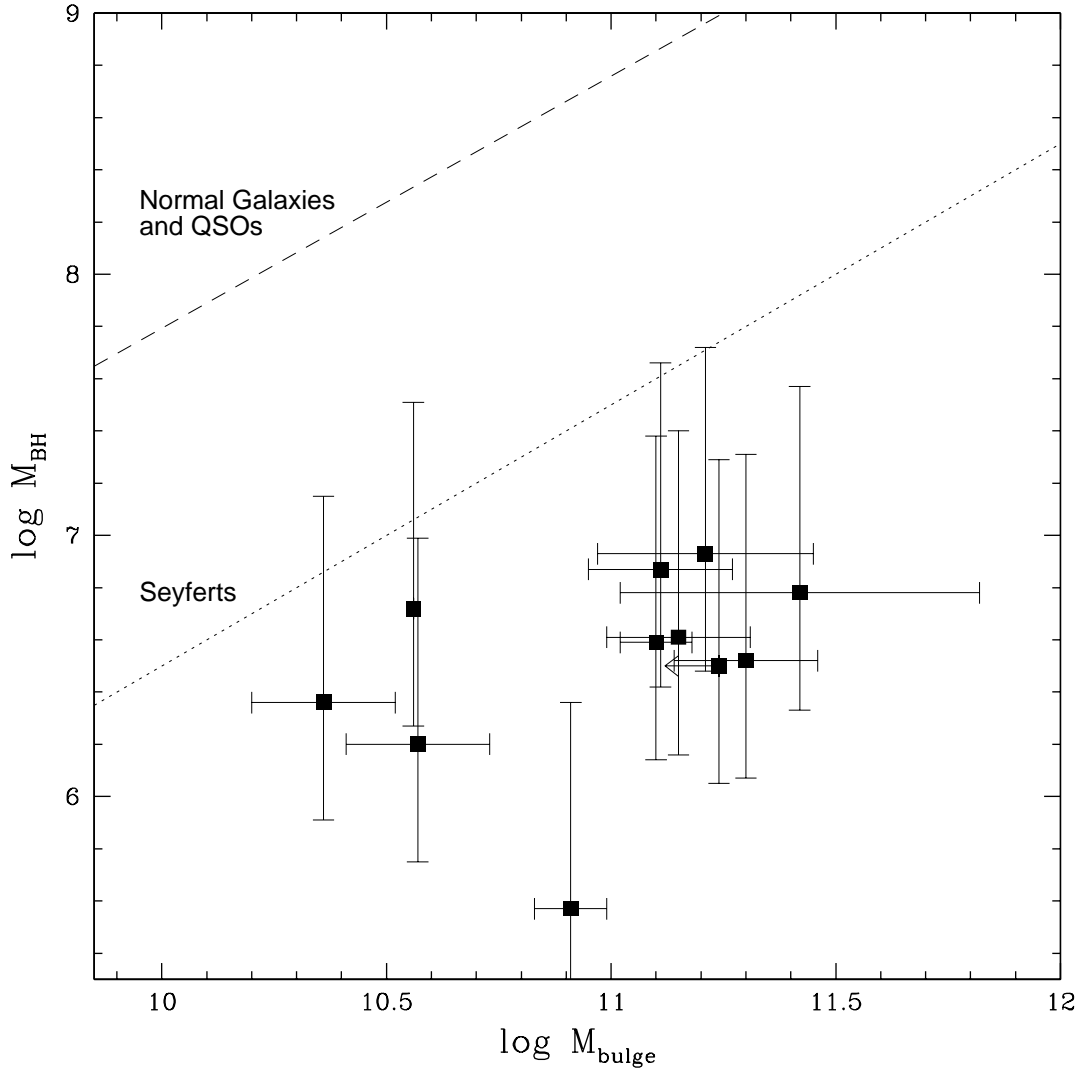


Fig. 2.—

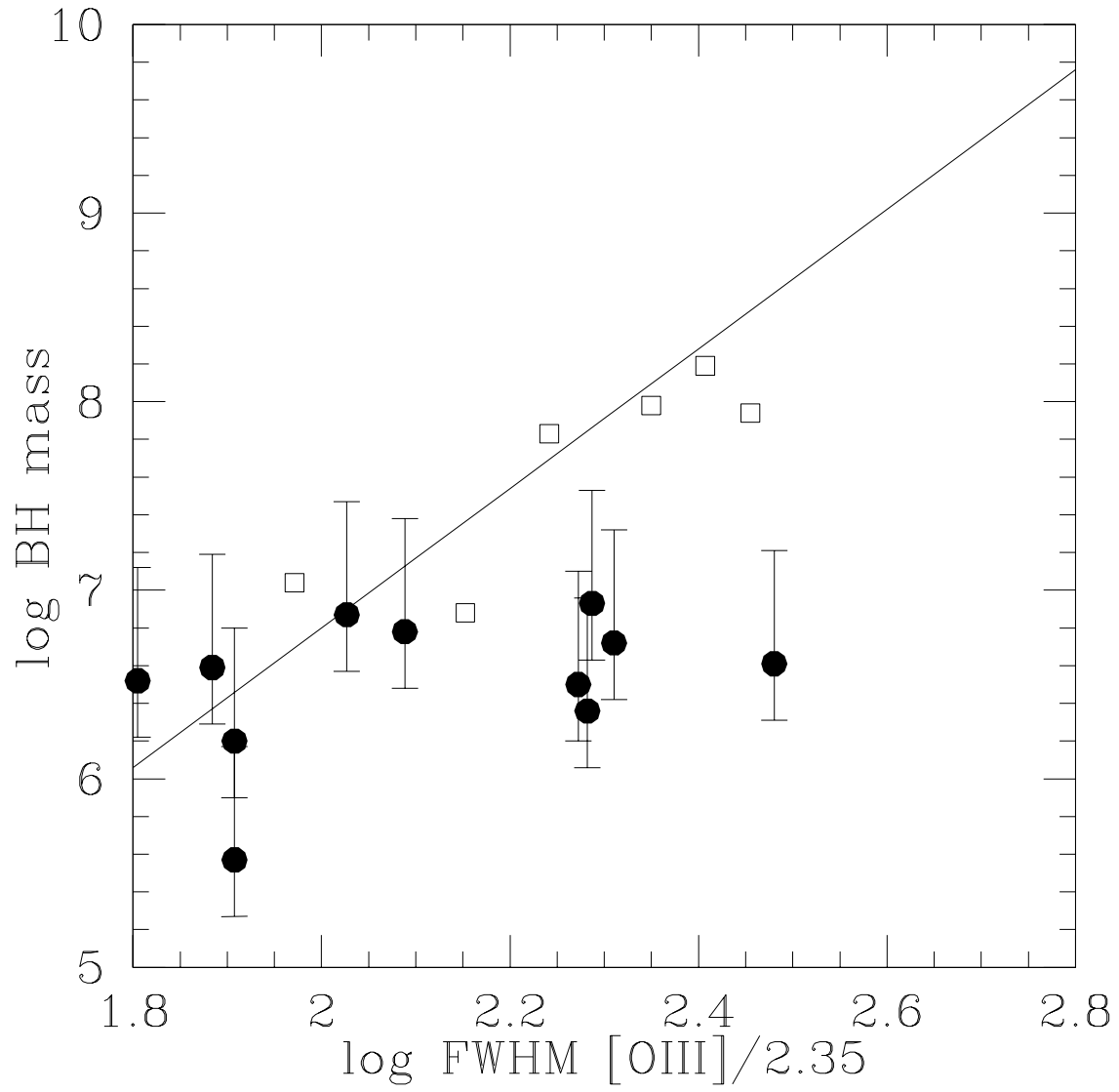


Fig. 3.—